

Lithium Diffusion & Magnetism in Battery Cathode Material $\text{Li}_x\text{Ni}_{1/3}\text{Co}_{1/3}\text{Mn}_{1/3}\text{O}_2$

M Månsson^{1,2}, H Nozaki³, J M Wikberg⁴, K Prša^{1,5}, Y Sassa⁵,
M Dahbi⁶, K Kamazawa⁷, K Sedlak⁸, I Watanabe⁹ and J Sugiyama³

¹ Laboratory for Quantum Magnetism, École Polytechnique Fédérale de Lausanne (EPFL),
CH-1015 Lausanne, Switzerland

² Lab. for Neutron Scattering & Imaging, Paul Scherrer Institute, CH-5232 Villigen PSI,
Switzerland

³ Toyota Central Research & Development Laboratories, Inc., 41-1 Yokomichi, Nagakute,
Aichi 480-1192, Japan

⁴ Department of Physics and Astronomy, Molecular and Condensed Matter Physics, Uppsala
University, Box 516, S-75120 Uppsala, Sweden

⁵ Laboratory for Solid state physics, ETH Zürich, CH-8093 Zürich, Switzerland

⁶ Department of Chemistry, Ångström Laboratory, Uppsala University, Box 538, S-75121
Uppsala, Sweden

⁷ Comprehensive Research Organization for Science and Society (CROSS), Tokai, Ibaragi
319-1106, Japan

⁸ Laboratory for Muon Spin Spectroscopy, Paul Scherrer Institute, CH-5232 Villigen PSI,
Switzerland

⁹ Advanced Meson Science Laboratory, RIKEN, 2-1 Hirosawa, Wako, Saitama 351-0198, Japan

E-mail: martin.mansson@epfl.ch

Abstract. We have studied low-temperature magnetic properties as well as high-temperature lithium ion diffusion in the battery cathode materials $\text{Li}_x\text{Ni}_{1/3}\text{Co}_{1/3}\text{Mn}_{1/3}\text{O}_2$ by the use of muon spin rotation/relaxation. Our data reveal that the samples enter into a 2D spin-glass state below $T_{\text{SG}} \approx 12$ K. We further show that lithium diffusion channels become active for $T \geq T_{\text{diff}} \approx 125$ K where the Li-ion hopping-rate $[\nu(T)]$ starts to increase exponentially. Further, $\nu(T)$ is found to fit very well to an Arrhenius type equation and the activation energy for the diffusion process is extracted as $E_a \approx 100$ meV.

1. Introduction

One of the main obstacles for a general breakthrough of electric automobiles is the development of a high-capacity, cheap and safe rechargeable battery. The most widely used cathode material is by far LiCoO_2 [1, 2], however, cobalt is very expensive and there is a strong driving force to find new cheaper and more environmental friendly cathode materials. One of the big problems for battery application is the structural distortions that occur [3, 4] when large amounts of Li is deintercalated during charge / discharge cycles of the battery [see Fig. 1]. Some efforts have been made to minimize these effects *e.g.* by combining Co and Ni into a $\text{LiNi}_{1-x}\text{Co}_x\text{O}_2$ solid solution. However, this compound suffers from strong intermixing of Ni into the Li layers for the highly delithiated state [5]. Recently, the mixed transition metal oxides (MTMO's) of the form $\text{Li}_x\text{Ni}_{1-y-z}\text{Co}_y\text{Mn}_z\text{O}_2$ have become the center of attention [6, 7]. In particular has the



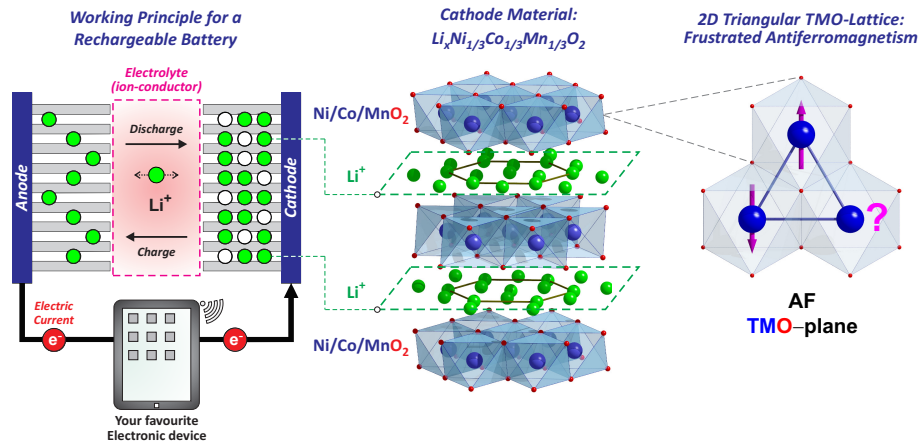


Figure 1. Schematic figure showing the operational principle for a standard rechargeable battery (left). Middle panel show the archetypical atomic structure for a layered battery cathode materials. Finally, right panel show the triangular transition metal oxide (TMO) planes that creates the possibility for 2D frustrated antiferromagnetism (AF) within the planes. This figure highlights that the very same layered TMO compounds can be of interest for energy applications as well as low-temperature fundamental condensed matter physics.

$\text{Li}_x\text{Ni}_{1/3}\text{Co}_{1/3}\text{Mn}_{1/3}\text{O}_2$ compound [8] been put forward as one of the most promising battery electrode materials for the future. The structure of these compounds is the same as for the fundamental LiCoO_2 i.e. a rhombohedral lattice (space group $R\bar{3}m$) where Ni/Co/MnO₂ planes are stacked between nonmagnetic Li layers along the c -axis [see Fig. 1]. In similarity with LiNiO_2 some intermixing of Ni in the Li layers can be expected. However, in this particular case, this actually helps to stabilize the structure and improve capacity retention [9].

In addition to their extensive use in energy related applications, these materials also display very interesting and complex magnetic properties at lower temperatures. This is due to the 2D triangular antiferromagnetic (AF) lattice [10] (see also Fig. 1) created by the transition metal ions. For the $\text{Li}_x\text{Ni}_{1/3}\text{Co}_{1/3}\text{Mn}_{1/3}\text{O}_2$ compounds the situation is even more complex since a combination of three different transition metals is present within the geometrically frustrated magnetic planes [11, 12, 13]. In this paper we have investigated both the low-temperature magnetic properties as well as the high-temperature ion-diffusion for two $\text{Li}_x\text{Ni}_{1/3}\text{Co}_{1/3}\text{Mn}_{1/3}\text{O}_2$ samples ($x = 1$ and 0.3) using muon spin rotation/relaxation ($\mu^+\text{SR}$).

2. Experimental Details

Powder samples of $\text{Li}_x\text{Ni}_{1/3}\text{Co}_{1/3}\text{Mn}_{1/3}\text{O}_2$ compound were prepared at Uppsala University, Sweden. For the low-temperature magnetic measurements, two samples ($x = 1$ and 0.3) of approximately 1 g each were sealed inside small envelopes made of very thin Al-coated Mylar tape under helium atmosphere and then attached to a low-background, fork-type, sample holder. Subsequently, high-resolution $\mu^+\text{SR}$ spectra were measured at the (continuous, DC) Swiss Muon Source ($S\mu\text{S}$), Paul Scherrer Institute, Villigen, Switzerland. By using the muon beamline πE1 with the Dolly spectrometer, zero-field (ZF) and weak transverse-field (wTF) spectra were collected for $2 \text{ K} \leq T \leq 150 \text{ K}$. For the ion-diffusion experiments, approximately 2 grams of the same samples were pressed into two discs with a 24 mm diameter and 1.5 mm thickness. Inside a helium glove-box the discs were packed into a Au-sealed (gold O-ring) powder cells made of pure titanium using a thin (100 μm) Kapton film as 'entrance window' for the muons. In addition, a silver mask with a hole matching the samples diameter was mounted onto the

cell to ensure that the any minor background signal is non-relaxing over a wide temperature range. The cell was mounted onto the Cu end-plate of a liquid-He flow-type cryostat in the temperature range between 10 and 500 K. Subsequently, ZF-, wTF- and LF- μ^+ SR spectra were collected using the RIKEN-RAL / ARGUS spectrometer at the pulsed muon source ISIS/RAL in UK. The experimental techniques are described in more detail elsewhere [14].

3. Results and Discussion: Low-temperature Magnetic Properties

To obtain a first insight into the nature of the magnetic order in these compounds, we acquired zero-field (ZF) data at the lowest temperature ($T = 2$ K). The μ^+ SR time spectrum show no indication of spontaneous muon precession, but rather only a fast exponentially decaying signal for both samples [see Fig. 2(a-b)]. Such signal indicate either a wide field-distribution, which is typical for spin-glasses (SG) or the presence of dynamical correlations. However, recent magnetometry measurements of our samples ($x = 1$ and $x = 0.3$) using zero-field-cooled (ZFC) and field-cooled (FC) protocols [15] clearly show a divergence around $T = 10$ K, which is a clear indication for a magnetically frustrated SG state. Further, information obtained also from related compounds using magnetometry as well as μ^+ SR [11, 12, 13] clearly favours the static SG scenario. The ZF data was found to be well fitted to the sum of a very fast exponentially relaxing signal and a slower decaying stretched-exponential function:

$$A_0 P_{ZF}(t) = A_{\text{fast}} \cdot e^{-\lambda_{\text{fast}} t} + A_{\text{slow}} \cdot e^{[-(\lambda_{\text{slow}} t)^n]}. \quad (1)$$

This kind of stretched exponential relaxation is found to appear in a range of different systems, however, they are commonly connected to SG systems [16] containing geometrical frustration *e.g.* the title compound. In similarity to our previous μ^+ SR studies of the closely related $\text{Li}(\text{Ni}_{0.8}\text{Co}_{0.1}\text{Mn}_{0.1})\text{O}_2$ compound [13], we find that also the present compounds enter into a disordered spin-glass (SG) state at lowest temperature ($T = 2$ K). Further, from the fits to Eq. 1 the critical exponent n reaches a value $n \leq 1/2$ [$n_{x=1} \approx 0.41$ and $n_{x=0.3} \approx 0.44$], possibly indicating a decreased dimensionality, however, this is only a phenomenological parametrisation of the data and other experimental methods needs to be employed. From ZF measurements at $T = 30$ K as well as $T = 100$ K it is evident that both samples are in a paramagnetic state above at least $T = 30$ K [see insets Fig. 2(a-b)].

To further investigate the PM to SG phase-transition we also performed detailed weak-transverse field (wTF = 50 G) measurements as a function of temperature. The wTF μ^+ SR time spectra for selected temperatures are shown in Fig. 2(c-d). Around $T = 10$ K a total suppression of the signal from the externally applied field is seen as annihilation of the wTF asymmetry (A_{TF}). The data is found to be well fitted by a combination of an exponentially relaxing cosine oscillation and a fast relaxing component (the latter becomes dominant at and below the transition):

$$A_0 P_{\text{TF}}(t) = A_{\text{TF}} \cos(2\pi f_{\text{TF}} \cdot t + \phi_{\text{TF}}) \cdot e^{-\lambda_{\text{TF}} t} + A_{\text{fast}} \cdot e^{-\lambda_{\text{fast}} t}. \quad (2)$$

From such fits, the temperature dependence of A_{TF} can be extracted and a better picture of the transition is obtained [Fig. 2(e-f)]. For both samples it is clear that a magnetic phase transition into the previously mentioned SG state occurs at $T_{\text{SG}} \approx 12$ K where A_{TF} drops to zero very rapidly. This is in fact rather different from the $\text{Li}(\text{Ni}_{0.8}\text{Co}_{0.1}\text{Mn}_{0.1})\text{O}_2$ compound [13] where we found a gradual transition over a 50 K wide temperature range. Hence, contrary to the cluster glass like state found for the previous compound, $\text{Li}_x\text{Ni}_{1/3}\text{Co}_{1/3}\text{Mn}_{1/3}\text{O}_2$ is believed to enter into a simple SG phase below T_{SG} . This could possibly be explained by the equal distribution of transition metals creating a higher degree of disorder on the TMO planes. Worth noticing is also that the $x = 1$ sample seems to have a slightly wider transition than $x = 0.3$. This could be an artefact related to too low statistics for the wTF data. Another explanation could be that stoichiometric $x = 1$ samples are well known to be notoriously difficult to synthesize.

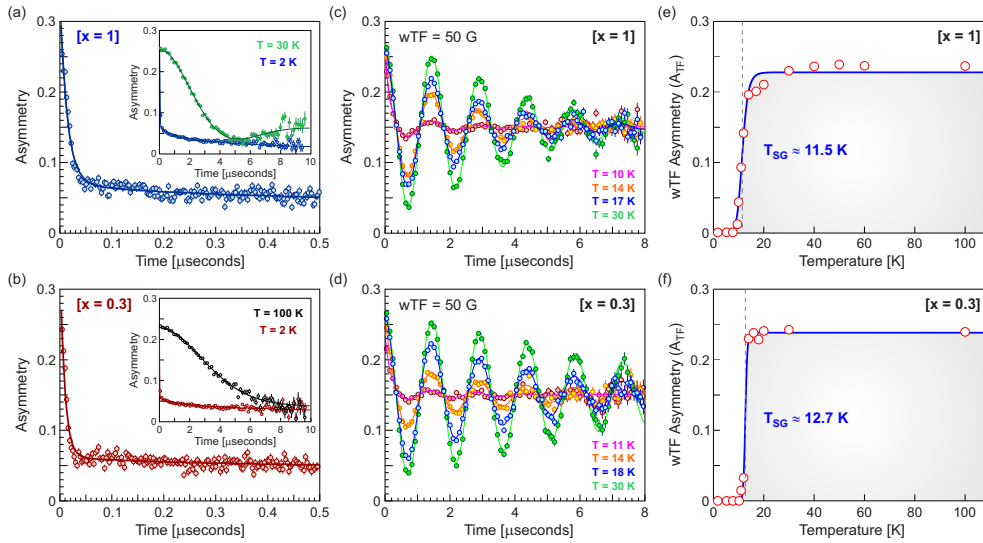


Figure 2. Low-temperature magnetic measurements at SμS continuous muon source. (a-b) Zero-field (ZF) μ^+ SR spectra at $T = 2$ K from the $x = 1$ and $x = 0.3$ samples, respectively. Data are shown in the very short time-scale in order to emphasize the fast relaxing signal. Solid line is a fit to Eq. 1. Insets show data in the longer time-scale together with a spectra at higher temperature, which in both cases display clear Kubo-Toyabe behaviour. (c-d) weak-transverse field (wTF = 50 G) data from the $x = 1$ and $x = 0.3$ samples, respectively, for a series of temperatures across the magnetic transition. Solid lines are fits to Eq. 2. (e-f) Temperature dependence of the wTF asymmetry (A_{TF}) from the two samples. A clear entrance into a magnetic state is observed in both cases for $T_{\text{SG}} \approx 12$ K.

4. Results and Discussion: High-temperature Li-ion Diffusion

In order to investigate Li-ion diffusion in these materials we have used our previously presented μ^+ SR technique for studying solid state ion diffusion in battery related materials [17, 18]. In similarity to our previous investigations of both Li-ion [17, 19, 20, 21, 22, 23, 24] and Na-ion [18] diffusion, a series of ZF, wTF = 30 G as well as LF = 5 G and 10 G μ^+ SR spectra were acquired in the temperature range between 50 and 500 K. At each temperature, the ZF and two LF spectra were fitted by an exponentially relaxing dynamic Kubo-Toyabe (KT) function plus a small background signal from the fraction of muons stopped mainly in the silver mask:

$$A_0 P(t) = A_{\text{KT}} G^{\text{DGKT}}(\Delta, \nu, t) \exp(-\lambda t) + A_{\text{BG}}. \quad (3)$$

Here the exponential relaxation of the KT is associated with the rapid electronic/paramagnetic fluctuations mainly from the TMO planes. Furthermore, a global fitting procedure was employed over the entire temperature range using a common alpha (α) and background asymmetry (A_{BG}), but with temperature dependent field fluctuation rate (ν). The static width of the local field distribution (Δ) and relaxation rate (λ) were from individual fitting found to be more or less independent of temperature and were finally also treated as common parameters for the global fit over the entire temperature range for each sample [$\Delta_{x=1} \approx 0.35 \cdot 10^6 \text{ s}^{-1}$ and $\Delta_{x=0.3} \approx 0.24 \cdot 10^6 \text{ s}^{-1}$ along with $\lambda \approx 0.025 \cdot 10^6 \text{ s}^{-1}$ for both samples].

Below $T \approx 120$ K, the spectra display a clear static behavior as shown for instance by the $T = 50$ K spectra for the $x = 1$ samples in Fig. 3(a) [except for the minor relaxation due to paramagnetic fluctuations as mentioned above]. However, above $T_{\text{diff}} \approx 125$ K clear dynamic contribution sets in, which increases strongly with temperature, as shown in the $T = 450$ K

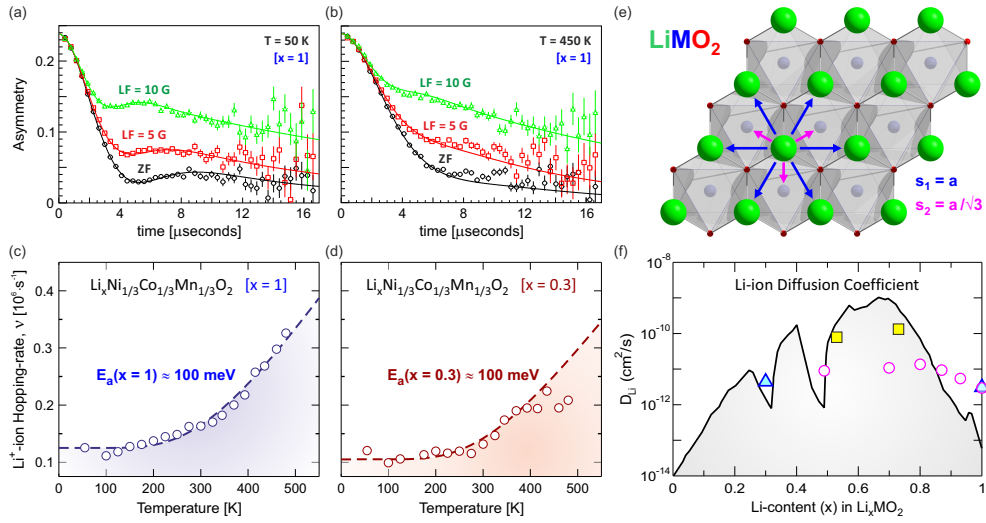


Figure 3. High-temperature diffusion measurements at ISIS pulsed muon source. Zero-field (ZF) and Longitudinal-field (LF = 5 and 10 G) μ^+ SR time spectra collected at (a) $T = 50$ K and (b) $T = 450$ K for the $x = 1$ sample. Solid lines are fits to Eq. 3. (c-d) Temperature dependence of the Li-ion hopping-rate [$\nu(T)$] obtained from our μ^+ SR experiments for $x = 1$ and $x = 0.3$ samples, respectively. (e) Li^+ -ion jump-paths and distances within the lithium planes. (f) Resulting Li-ion diffusion coefficient (D_{Li}) for the current two $\text{Li}_x\text{Ni}_{1/3}\text{Co}_{1/3}\text{Mn}_{1/3}\text{O}_2$ samples shown as filled blue triangles. Also shown are results from previous μ^+ SR measurements on similar samples with different x [25] (open circles) as well as from the Li_xCoO_2 compound [17] (filled yellow squares) together with a calculated curve for D_{Li} in Li_xCoO_2 as solid black line [3].

spectra for the $x = 1$ sample [Fig. 3(b)]. The temperature dependence of the Li-ion hopping rate [$\nu(T)$] obtained from fitting both data sets to Eq. 3 are shown in Fig. 3(c-d) for the $x = 1$ and $x = 0.3$ samples, respectively. As seen, $\nu(T)$ displays a clear diffusive behavior above $T_{\text{diff}} \approx 150$ K for both samples. By fitting $\nu(T)$ to an Arrhenius type equation [dashed line in Fig. 3(c-d)], it is possible to extract the activation energy $E_a \approx 100$ meV for both samples. As seen in Fig. 3(d), for the $x = 0.3$ sample there is a small deviation at higher temperatures. One could argue that this is due to the onset of muon diffusion in parallel to the Li-ion diffusion. However, this is highly unlikely since then a similar effect could be expected also for the $x = 1$ sample. Instead we attribute this feature to the fact that this was the last sample we measured and had to cut down on the statistics for the last couple of temperature points. If we assume that $\nu(T)$ is a direct measure of the Li-ion hopping rate we can then express the diffusion coefficient D_{Li} as [26]:

$$D_{\text{Li}} = \sum_{i=1}^n \frac{1}{N_i} Z_i s_i^2 \nu. \quad (4)$$

Here, N_i is the number of possible Li jump sites for the i :th path, Z_i is the vacancy fraction, s_i is the jump distance and ν is the hopping rate obtained from our μ^+ SR experiments. For the current samples there are in similarity to Li_xCoO_2 samples 2 different jumping paths to either a partly occupied Li-ion site ($N_1 = 6$, $Z_1 = 1 - x$ and $s_1 = \mathbf{a}$ -axis = $2.86347(2)$ Å) or to an empty interstitial site ($N_2 = 3$, $Z_2 = 1$ and $s_2 = \mathbf{a}$ -axis/ $\sqrt{3}$) [see also Fig. 3(e)]. As a result we can calculate D_{Li} at 300 K for our two samples as $D_{\text{Li}}^{300\text{K}}[x = 1] = 3.5 \cdot 10^{-12} \text{ cm}^2\text{s}^{-1}$ and

$D_{\text{Li}}^{300\text{K}}[x = 0.3] = 5 \cdot 10^{-12} \text{ cm}^2\text{s}^{-1}$, respectively. If we insert such values in a graph showing D_{Li} from previous measurements of $\text{Li}_x\text{Ni}_{1/3}\text{Co}_{1/3}\text{Mn}_{1/3}\text{O}_2$ samples [25] we clearly see that the value for $x = 1$ is fully reproducible. Our new data for $x = 0.3$ falls where one can expect considering the previous measurements of $x = 0.49$ samples. Please note that a different sample provider was used for the current study as compared to previously published data [25].

An interesting detail appears when looking at the first principle calculations for D_{Li} in the closely related Li_xCoO_2 compound [3] [see solid black line in Fig. 3(f)], several sharp minima at *e.g.* $x = 0.33$ and $x = 0.5$ are visible. Such minima are related to different type of Li-vacancy ordering. However, from the present and previous measurements on $\text{Li}_x\text{Ni}_{1/3}\text{Co}_{1/3}\text{Mn}_{1/3}\text{O}_2$ for a series of different Li-content, x , it seems clear that no such minima are present in this compound. This is probably reasonable since the disorder in the MTMO planes would create an unfavorable environment for the spontaneous formation of any Li-vacancy ordering. Such disorder is most likely also the cause for the overall lower diffusion rate in the MTMO compared to the LiCoO_2 compound causing for instance the interstitial sites to be less favourable. Another possibility is that we have an intermixing between the Li and Ni sites. As we have already found from our previous measurements on the LiNiO_2 compound [19] the diffusion rate is drastically lowered if such intermixing is present. To reveal the details of such issues we will need to perform further measurements using *e.g.* neutron diffraction and/or quasi-elastic neutron scattering (QENS).

5. Summary

By the use of a positive muon-spin rotation and relaxation ($\mu^+\text{SR}$) technique we have investigated the mixed transition metal oxide battery cathode material $\text{Li}_x\text{Ni}_{1/3}\text{Co}_{1/3}\text{Mn}_{1/3}\text{O}_2$. Low-temperature ($T = 2 - 100$ K) measurements show that this compounds enters into a spin-glass like magnetic state below approximately $T = 12$ K for both lithium contents $x = 1$ and $x = 0.3$, respectively. High-temperature ($T = 50 - 500$ K) investigations show details regarding the Li-ion diffusion process in these compounds. Above $T_{\text{diff}} \approx 125$ K the lithium ions start to diffuse as seen from the exponential increase of the hopping rate $\nu(T)$. We are able to extract the activation energy for the diffusion mechanism as $E_a \approx 100$ meV, which seems to be approximately independent of the lithium content x .

Acknowledgments

This work was performed using the DOLLY spectrometer at the Swiss Muon Source ($S\mu S$) of the Paul Scherrer Institut (PSI), Villigen, Switzerland as well as the RIKEN-RAL / ARGUS spectrometer at the pulsed muon source ISIS/RAL in UK. We are very grateful for the support obtained during our experiments from the beamline and technical staff of the two facilities. This research was financially supported by the Swedish Research Council (VR), Swedish Energy Agency, Knut and Alice Wallenberg Foundation (KAW), the Swiss National Science Foundation (SNSF), MEXT KAKENHI Grant No. 23108003 and JSPS KAKENHI Grant No. 26286084.

References

- [1] Mizushima K, Jones P C, Wiseman P J and Goodenough J B 1980 *Mater. Res. Bull.* **15** 783
- [2] Li H, Wang Z, Chen L and Huang X 2009 *Adv. Mater.* **21** 4593
- [3] Van der Ven A, Aydinol M K, Ceder G, Kresse G and Hafner J 1998 *Phys. Rev. B* **58** 2975
- [4] Seguin L, Amatucci G, Anne M, Chabre Y, Strobel P, Tarascon J M and Vaughan G 1999 *J. Power Sources* **81/82** 604
- [5] Chebiam R V, Prado F and Manthiram A 2001 *J. El. Chem. Soc.* **148** A49
- [6] Yoshio M, Noguchi H, Itoh J -I, Okada M and Mouri T 2000 *J. Pow. Sour.* **90** 176
- [7] Choi J and Manthiram A 2006 *J. Pow. Sour.* **162** 667
- [8] Ohzuku T and Makimura Y 2001 *Chem. Lett.* **7** 642
- [9] Dahbi M, Wikberg J M, Saadoune I, Gustafsson T, Svedlindh P and Edström K 2009 *Electrochimica Acta* **54** 3211

- [10] Anderson P W 1973 *Mater. Res. Bull.* **8**, 153
- [11] Wikberg J M, Dahbi M, Saadoune I, Gustafsson T, Edström K and Svedlindh P 2010 *Phys. Rev. B* **81** 224411
- [12] Wikberg J M, Dahbi M, Saadoune I, Gustafsson T, Edström K and Svedlindh 2010 *J. Appl. Phys.* **180** 083909
- [13] Wikberg J M, Månsson M, Dahbi M, Kamazawa K and Sugiyama J 2012 *Phys. Proc.* **30** 202
- [14] Yaouanc A and Dalmas de Réotier P 2011 *Muon Spin Rotation, Relaxation, and Resonance* (Oxford: Oxford University Press)
- [15] Wikberg J M 2014 *Private Communication*
- [16] Phillips C 1996 *Rep. Prog. Phys.* **59** 1133
- [17] Sugiyama J, Mukai K, Ikedo Y, Nozaki H, Månsson M and Watanabe I 2009 *Phys. Rev. Lett.* **103** 147601
- [18] Månsson M and Sugiyama J 2013 *Physica Scripta* **88** 068509
- [19] Sugiyama J *et al.* 2010 *Phys. Rev. B* **82** 224412
- [20] Sugiyama J *et al.* 2011 *Phys. Rev. B* **84** 054430
- [21] Sugiyama J *et al.* 2012 *Phys. Rev. B* **85** 054111
- [22] Sugiyama J, Mukai K, Nozaki H, Harada M, Månsson M, Kamazawa K, Andreica D, Amato A, and Hillier A D 2013 *Phys. Rev. B* **87**, 024409
- [23] Sugiyama J, Nozaki H, Mukai K, Harada M, Månsson , and Hillier A 2014 *Solid State Ionics* **262** 901
- [24] Sugiyama J *et al.* 2012 *Phys. Proc.* **30** 105
- [25] Sugiyama J, Mukai K, Harada M, Nozaki H, Miwa K, Shiotsuki T, Shindo Y, Giblin S R and Lord J S 2013 *Phys. Chem. Chem. Phys.* **15** 10402
- [26] Borg R J and Dienes G J 1988 *An Introduction to Solid State Diffusion* (San Diego: Academic)